

# Six Higgs Doublets Model for Dark Matter

**Mohammad Alakhras<sup>1\*</sup>, Nidal Chamoun<sup>2,4†</sup>, Xue-Lei Chen<sup>3‡</sup>, Chao-Shang Huang<sup>4§</sup> and Chun Liu<sup>4¶</sup>**

<sup>1</sup> Department of Physics, Faculty of Sciences, Damascus University, Damascus, Syria.

<sup>2</sup> Physics Department, HIAST, P.O.Box 31983, Damascus, Syria.

<sup>3</sup> Key Laboratory of Computational Astrophysics, National Astronomical Observatories, CAS, Beijing 100012, China.

<sup>4</sup> CAS Key Laboratory of Theoretical Physics, Institute of Theoretical Physics, CAS, P.O. Box 2735, Beijing 100190, China.

October 4, 2018

## Abstract

We consider an extension of the Higgs sector in the standard model (SM) with six Higgs doublets. The gauge couplings are unified without supersymmetry in this model. The lightest of the extra Higgs particles, being stabilized by a discrete symmetry imposed from the outset, presents a plausible candidate for dark matter. For a specific acceptable benchmark point, we show that the model is viable regarding the constraints of relic density, direct detection and invisible Higgs decay. We comment on the mean free path of the dark matter candidate.

## 1 Introduction

As is well known, baryonic matter constitutes only 4-5% of the total cosmic energy density. About 20% of the Universe is made up of dark matter (DM), and the remaining part is dark energy [1]. Although the first evidence of DM was found seven decades ago, we still do not know its composition, and finding clues for its nature is one of the most pressing issues in physics. Since none of the particles in the Standard Model (SM) can be a viable candidate of the major part of the DM, a successful extension of the SM of particle physics is likely to address this problem. Interestingly, Weakly Interacting Massive Particles (WIMPs) can be very good candidates of the cold DM (CDM), since their relic abundances agree naturally with astrophysical observations. Many particle physics models were proposed involving new, other than SM, particles having masses at the weak scale, and which couple weakly to the SM particles.

In supersymmetric (SUSY) models with  $R$ -parity conservation, the lightest SUSY particle (LSP) is stable, and is a DM candidate. The most popular LSP is the neutralino, a superposition of photino, zino and the two Higgsinos. The experimental limit on the mass of the lightest neutralino,  $\tilde{\chi}_1^0$ , due to the negative searches at accelerators such as LHC, is  $m_{\tilde{\chi}_1^0} > 46$  GeV [2]. Other possible SUSY DM candidates include gravitino and sneutrino.

Moreover, SUSY allows also for coupling unification of the strong, weak, and electromagnetic interactions, and pushes the unification scale in  $SU(5)$  models from  $10^{15}$  GeV in its absence up to around  $10^{16}$  GeV. This likely makes the  $SU(5)$  GUT safe from rapid proton decay [3]\*.

Although well motivated, SUSY models are theoretically quite complicated. Moreover, the negative searches for its simple versions at the LHC impose stiff constraints on SUSY models. In fact, there are other ways to achieve gauge coupling unification. Upon closer examination of SUSY models, the

\*m.alakhras@damasuniv.edu.sy

†nchamoun@th.physik.uni-bonn.de

‡xuelei@cosmology.bao.ac.cn

§csh@itp.ac.cn

¶liuc@mail.itp.ac.cn

\*The minimal SUSY  $SU(5)$  has been already excluded by the limit  $(6.7 \times 10^{32} \text{ y})$  of the proton lifetime from Super Kamiokande [4]. Nevertheless, there are a number of ways in which this limit can be satisfied (for a review, see [5])

modification on the running of the gauge coupling is due entirely to the extension of the Higgs sector, which includes a second Higgs doublet and the corresponding superpartners. It has been known that the unification of the gauge couplings can also be achieved without SUSY, if the SM has an extended Higgs sector with six Higgs doublets at the weak scale [6]. Furthermore, the problem of rapid proton decay can be tamed in non-SUSY extended Higgs models, such as the trinification model [7], where the GUT gauge group is not a simple group but the product group  $SU(3)_C \times SU(3)_L \times SU(3)_R \times Z_3$ , and where the proton life time can be above the experimental limits [8].

For the non-SUSY gauge unification model, a very interesting question arises as to whether or not this model can provide an explanation for the DM problem. Various non-SUSY models for DM were proposed ranging from axions [9], sterile neutrinos [10], to lightest Kaluza-Klein excitations in universal extra dimensions models [11], and/or branons where the fluctuations of the branes in string theory can be made into suitable CDM candidates [12]. SM-singlet extensions [13, 14] are popular DM models. The additional SM-singlet scalars have no direct coupling to gauge fields, and so no annihilation into gauge bosons unless via intermediate Higgs. Thus these models are mainly Higgs-portal models. Since the SM Higgs sector is based on doublets, one can consider another way going beyond SM by extending the Higgs sector. Here, the DM can be accommodated considering certain combinations of the additional doublets, and the DM direct annihilations into gauge vector bosons exist leading to known signatures compared to singlet extensions. The inert Doublet Model (IDM) [15, 16], where one adds another ‘inert’ doublet to the SM Higgs doublet, is a starting point for many extensions, can accommodate axions while still being testable experimentally [17], and has been suggested as a simple and yet rich model for DM [18, 19].

In this work we study the DM problem within the framework of multi-doublet scalars without SUSY. In particular, we extend the SM Higgs sector to contain six Higgs doublets, and consider the possibility of one of the ‘additional’ Higgs particles being the DM. We show that if one imposes a discrete symmetry, then one of the Higgs particles can be stabilized, thus providing a possible candidate of DM. Thus, extending the Higgs sector in a non-SUSY context helps to realize two objectives: gauge unification and accounting for DM. More specifically, we assume that two of the Higgs doublets ( $H_u, H_d$ ) get vacuum expectation values (VEV), to break the electroweak symmetry and generate masses for the quarks and charged leptons. This part of the model is similar to the two Higgs doublet model (2HDM) [20, 21] and is phenomenologically viable [22, 23]. For simplicity, we call hereafter this part the “active doublets” whereas we call the remaining part the “inert doublets”. We denote the lightest neutral component of the additional Higgs particles (LAH), in inert doublets, by  $\psi$  which, due to the discrete symmetry imposed, can not decay to SM Higgses ( $H_u, H_d$ ), nor can it have Yukawa-type interactions.

Actually, DM with one Higgs ‘active’ doublet plus two ‘inert’ doublets (denoted 1+2), considered the simplest extension to the DM with (1+1) IDM, was studied in [24, 25] and shown to have a richer phenomenology than the IDM or the (2+0) 2HDM. Motivated by SUSY which requires an even number of doublets, the authors of [24] extended the (1+2) model into a (2+4) model with two Higgs active doublets and four inert doublets, and computed the mass spectrum of the model for a special form of the Lagrangian  $\mathcal{L}_0$ .

Besides this heuristic argument in going from the IDM (1+1) to the (2+4) passing through (1+2), we note moreover that although the LHC Higgs is SM-like, however many approaches posses a decoupling limit behaving like the SM, and the 2HDM provides a framework for studying the decoupling limit and possible departures from SM-like Higgs behavior [26].

We thus take the same (2+4) extension motivated, in addition, by the unification of coupling constants plus accounting for DM, and we build it with the most general form of the Lagrangian, containing  $\mathcal{L}_0$  of [24], allowed by symmetry. We did not consider the (1+5) extension as it resembles the (1+1) IDM except for having more particles some of which may be close in mass to the DM mass, and thus more possible co-annihilation channels exist. The extension (2+4) is far richer since, compared to the SM, we changed both the inert and the active sectors. In fact, the 2HDM is chosen rather than the SM because it is under scrutiny at present in view of the LHC results [27], and it is a simple extension of the SM.

For the phenomenological analysis, and since we focus in this work on the model building and its feasibility for providing a DM candidate, we took a special benchmark point in the parameter space, called “symmetric choice”, which mimics the case rarely studied of the (2+1) model. In this simplest realization, the model will have three free parameters: the mass of the new LAH  $m_\psi$ , a dimensionless

self-coupling  $\lambda_S$  and a dimensionless coupling  $\lambda$  to the SM Higgs ( $H$ ). If the LAH is the DM, then  $\lambda$  and  $m_\psi$  are related by requiring it to give the cosmological DM abundance. In addition to the Relic Density (RD) constraint, we imposed also the constraints originating from the Invisible Higgs Decay (IHD) and the negative searches of the Direct Detection (DD) experiments related to the DM elastic scattering with atomic nuclei. We find that the mass of the LAH should be around the Higgs resonance ( $m_\psi \approx \frac{1}{2}m_H$ ) in order to have a perturbative coupling ( $\lambda \leq 1$ ), to account for the DM abundance and to respect the IHD and DD constraints. As a matter of fact, the authors of [28] studied the extension (2+1) where an inert doublet was added to the 2HDM, and explored the  $CP$  violation effects in it. However, no IHD constraints were considered there, and no phenomenology relating the DM mass versus the coupling  $\lambda$  between the active and inert Higgs doublets was presented. Moreover, we have taken into account the new updated experimental constraints, and in particular we have imposed the newly discovered Higgs mass value.

In this work we have computed the scattering/decay amplitudes using the Mathematica packages (SARAH, FeynArts, FormCalc) [29], and then obtained the thermal relic abundance by using approximate formulae[30, 31]. This enables us to see the details of the various processes, and is sufficient for checking the basics of the model. The more sophisticated package such as micrOMEGAs [32], while more complete and accurate, hides much physical details under its hood. However, we checked that for the chosen benchmark point of parameter space considered here, the micrOMEGAs package gives results in line with what we get here.

The paper is organized as follows. In section 2, we review the gauge coupling unification with six Higgs doublets in subsection (2.1), and build our (2+4) model presenting the most general form of the Lagrangian in subsection (2.2). We implement sufficient conditions for the stability of the potential in subsection (2.3). In subsection (2.4) we present the sector representing the active Higgs doublets, whereas subsection (2.5) presents the inert sector. Section 3 is devoted to our “symmetric choice” benchmark point stated in subsection (3.3). In subsections (3.1, 3.2) we determine the parameter space point in the active and inert sectors respectively. We present the phenomenological analysis in section 4. Subsection (4.1) presents the RD computations, whereas subsection (4.2) presents the DD constraints. Subsection (4.3) presents the IHD constraints, and finally we comment on the DM self-elastic scattering in subsection (4.4). Section (5) presents our conclusions about the viability of the model in the “symmetric choice” benchmark point. There are few appendices where several technical formulae are listed.

## 2 Building the Model

### 2.1 Motivation–Unification of gauge couplings

In order to achieve gauge unification in the model, let us review how this is done in the SUSY  $SU(5)$  model. The fermion superpartners in the SUSY model do not affect the relative evolution of the gauge couplings, since they fall in complete representations of the  $SU(5)$  group, while the boson superpartners change the unification scale. Crucially, it is the existence of second Higgs doublets, as well as the Higgs superpartners which modifies the relative evolution of the gauge couplings, because the Higgs doublets do not form a complete representation of the  $SU(5)$  group.

The renormalization group equation for the gauge couplings  $\alpha_k = \frac{g_k^2}{4\pi}$ , reads:

$$\frac{1}{\alpha_k(\mu)} - \frac{1}{\alpha_k(\mu')} = \frac{b_k}{2\pi} \ln \left( \frac{\mu'}{\mu} \right), \quad (1)$$

where the  $b_k$ ’s are the beta-functions given by

$$\frac{dg_k}{d \log \mu} \equiv \beta_k(g_k) \equiv \frac{\beta_{g_k}^{(1)}}{(4\pi)^2} + \frac{\beta_{g_k}^{(2)}}{(4\pi)^4} = b_k \frac{g_k^3}{(4\pi)^2} + \sum_{\ell=1}^{\ell=3} b_{k\ell} \frac{g_k^3 g_\ell^2}{(4\pi)^4} + \frac{g_k^3}{(4\pi)^4} \text{Tr} \left( C_\ell^u Y_u Y_u^\dagger + C_\ell^d Y_d Y_d^\dagger + C_\ell^e Y_e Y_e^\dagger \right) \quad (2)$$

In appendix A, we find the following expressions:

$$\beta_{g_1}^{(1)} = \frac{23}{5} g_1^3 \quad (3)$$

$$\beta_{g_1}^{(2)} = \frac{1}{50} g_1^3 \left( 244g_1^2 - 25\text{Tr}(Y_d Y_d^\dagger) + 360g_2^2 + 440g_3^2 - 75\text{Tr}(Y_e Y_e^\dagger) - 85\text{Tr}(Y_u Y_u^\dagger) \right) \quad (4)$$

$$\beta_{g_2}^{(1)} = -\frac{7}{3} g_2^3 \quad (5)$$

$$\beta_{g_2}^{(2)} = \frac{1}{30} g_2^3 \left( -15\text{Tr}(Y_e Y_e^\dagger) + 360g_3^2 - 45\text{Tr}(Y_d Y_d^\dagger) - 45\text{Tr}(Y_u Y_u^\dagger) + 500g_2^2 + 72g_1^2 \right) \quad (6)$$

$$\beta_{g_3}^{(1)} = -7g_3^3 \quad (7)$$

$$\beta_{g_3}^{(2)} = -\frac{1}{10} g_3^3 \left( -11g_1^2 + 20\text{Tr}(Y_d Y_d^\dagger) + 20\text{Tr}(Y_u Y_u^\dagger) + 260g_3^2 - 45g_2^2 \right) \quad (8)$$

We plot in Fig. 1 the 1-loop (left) and 2-loop (right) running couplings for the particle content of the SM but with 6 Higgs doublets, and with the inputs  $\alpha_3(M_Z) = 0.117$ ,  $\alpha_2(M_Z) = (\sqrt{2}/\pi)G_F M_W^2 = 0.034$  and  $\alpha_1(M_Z) = (5/3)\alpha_2(M_Z) \tan^2 \theta_W = 0.017$ . We limited the Yukawas couplings to the third family and did not consider the “higher order” effect of the masses’ running, so took, say,  $\text{Tr}Y_u Y_u^\dagger = 2\frac{m_t^2}{v^2} \approx 2(\frac{175}{246})^2$ . We see the 2-loop unification is better satisfied than that of the 1-loop, and that the unification scale occurs at around  $M_U \sim 10^{13.7}$  GeV. This low unification scale yields rapid proton decay in conventional  $SU(5)$  theory. In order to avoid this problem, we consider, as Ref. [8, 6], the possibility that the unified theory is not  $SU(5)$  but a trinified model based on  $SU(3)_C \times SU(3)_L \times SU(3)_R \times Z_3$ , with a Higgs sector containing six <sup>†</sup> Higgs fields in the 27-dim representation of  $(SU(3))^3$ . Those fields, upon symmetry breaking

$$(SU(3))^3 \rightarrow SU(3)_c \times SU(2)_L \times U(1)_Y,$$

leads to the SM with six Higgs doublets, of which one linear combination acquires a mass of order of the unification scale while the remaining five doublets may have the mass of order of the weak scale [8]<sup>‡</sup>.

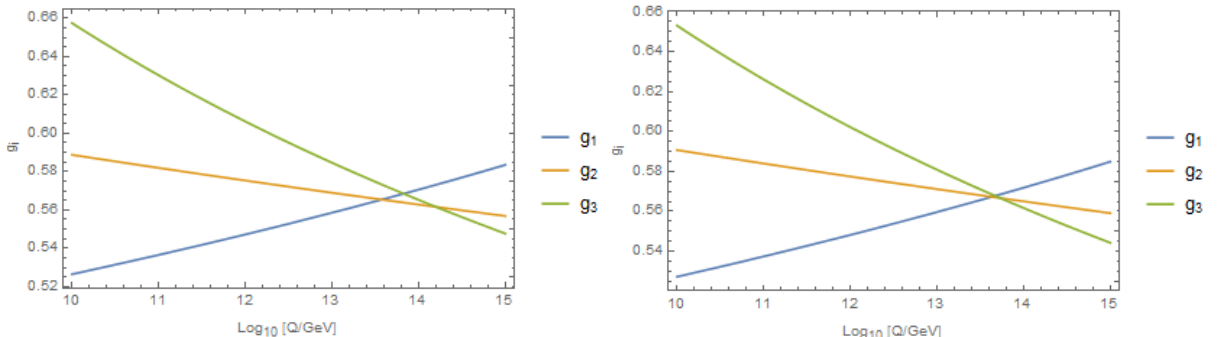


Figure 1: Unification of gauge couplings in SM with  $n_H = 6$  Higgs doublets at 1-loop (left) and 2-loop (right) runnings.

## 2.2 The Lagrangian

We denote the six Higgs fields of hyper charge  $Y = 1$  by  $H_I (I = u, d)$ ,  $H_\alpha (\alpha = 1, \dots, 4)$ . The electroweak symmetry is broken to  $U(1)_{em}$  when any of the six Higgs doublets acquires an electroweak scale VEV. For simplicity, we follow [8] and assume that two such Higgses ( $H_I (I = u, d)$ ) get VEVs:  $H_u$  to give masses to the u-type quarks and  $H_d$  to give masses to the d-type quarks and to the charged leptons. This parallels the structure of the known two-Higgs doublet model (type II). In order to naturally suppress flavor

<sup>†</sup>In fact, one can get gauge unification with either five or six Higgs doublets. However, to keep with the model triplication paradigm, we assume six such Higgses.

<sup>‡</sup>The work of [33] also considered SM with 6 Higgs doublets and showed that with an invisible axion it is possible to obtain proton stability and coupling unification at an energy near the Peccei-Quinn scale.

changing neutral currents, i.e., to have natural flavor conservation (NFC), one imposes some discrete symmetry and a simplest choice is a  $Z_2$  symmetry:

$$H_u \rightarrow -H_u, \quad u_R \rightarrow -u_R \quad (9)$$

and all the other fields unchanged under the  $Z_2$  transformation. To keep at least one of the other Higgses stable, we impose another discrete symmetry  $Z'_2$  under which  $H_\alpha \rightarrow -H_\alpha$  ( $\alpha = 1, \dots, 4$ ) while all other fields are unchanged.

The general form of the renormalizable  $SU(2)_L \times U(1)_Y$  gauge invariant Lagrangian which is invariant under the discrete symmetry  $Z_2 \times Z'_2$  is given by:

$$\mathcal{L} = \mathcal{L}_{\text{Kin}} - V(H) - V_{\text{Yuk}} \quad (10)$$

where:

$$\mathcal{L}_{\text{Kin}} = (D_\mu H_I)^\dagger (D_\mu H_I) + (D_\mu H_\alpha)^\dagger (D_\mu H_\alpha) \quad (11)$$

$$V(H) = V_{\text{Active}} + V_{\text{Inert}} + V_{\text{Coupled}} \quad (12)$$

$$V_{\text{Active}} = \mu_{II} H_I^\dagger H_I + \lambda_{IIJJ} H_I^\dagger H_I H_J^\dagger H_J + \left( \eta_{IJJI} H_I^\dagger H_J H_J^\dagger H_I \right. \quad (13)$$

$$\left. + \frac{1}{2} \left( \xi_{IJJJ} H_I^\dagger H_J H_J^\dagger H_I + h.c. \right) \right)_{I \neq J} \quad (14)$$

$$V_{\text{Inert}} = \mu_{\alpha\beta} H_\alpha^\dagger H_\beta + \lambda_{\alpha\beta\gamma\delta} H_\alpha^\dagger H_\beta H_\gamma^\dagger H_\delta + h.c. \quad (15)$$

$$V_{\text{Coupled}} = \lambda_{II\alpha\beta} H_I^\dagger H_I H_\alpha^\dagger H_\beta + \eta_{I\alpha\beta I} H_I^\dagger H_\alpha H_\beta^\dagger H_I + \frac{1}{2} \left( \xi_{I\alpha I\beta} H_I^\dagger H_\alpha H_\beta^\dagger H_I + h.c. \right), \quad (16)$$

$$V_{\text{Yuk}} = Y_l L^\dagger H_d e_R + Y_d Q H_d d_R + Y_u Q \tilde{H}_u u_R \quad (17)$$

with  $\tilde{H}_u = i\tau_2 H_u^*$ , the covariant derivative  $D_\mu = \partial_\mu + igW^{I\nu} \frac{\sigma^I}{2} g_{\mu\nu} + ig'B^\nu g_{\mu\nu}$ , and the  $W$  and  $B$  are the gauge bosons for  $SU(2)_L \times U(1)_Y$ , and where the Latin indices ( $I, J$ ) run over the set  $\{u, d\}$ , whereas the Greek indices ( $\alpha, \beta$ ) span the set  $\{1, \dots, 4\}$ .

Before proceeding some remarks are in place. First, from the Lagrangian (10), the lightest among the additional Higgses (LAH), say, the neutral component  $\psi$  of  $(H_3)^t \equiv (H_\alpha^+, \phi_3 + i\sigma_3)$ , is stable since it can not decay to other particles, and thus is a possible candidate for the DM. Our restriction that  $H_I$ 's only have a non-zero electroweak VEV means that the  $Z'_2$  symmetry is unbroken after the electroweak symmetry breaking. If one, instead of  $Z'_2$ , imposes a symmetry  $R$  of a reflection on each additional Higgs doublet, i.e.  $R = \prod_{\beta=1}^{\beta=4} Z_2^{(\beta)}$  where under each  $Z_2^{(\beta)}$  we have  $H_\beta \rightarrow -H_\beta$  whereas all the other fields are unchanged, then we have [34, 35]:

$$V(H) = \sum_i [\mu_i H_i^\dagger H_i + \lambda_{ii} (H_i^\dagger H_i)^2] + \sum_{i < j} [\lambda_{ij} H_i^\dagger H_i H_j^\dagger H_j + \eta_{ij} H_i^\dagger H_j H_j^\dagger H_i + (\xi_{ij} H_i^\dagger H_j H_i^\dagger H_j + h.c.)] \quad (18)$$

where  $i \in \{u, d, 1, \dots, 4\}$ . In this situation, the lighter of neutral Higgs bosons for each additional doublet is stable and can be a candidate for the DM. For simplicity we do not pursue this case in the paper. Next, if all coupling constants are real the potential is CP-invariant. There is also no spontaneous CP breaking because we have assumed that only two doublets of all the six doublets can get non-zero vevs and there are no linear terms of the form  $H_u^+ H_d$  due to the  $Z_2$  symmetry. We do not discuss CP violation in the paper so that we assume all couplings are real hereafter. Third, as it is obvious from the potential (12) (as well as (18)), we do not have a Peccei-Quinn  $U(1)$  global symmetry, and thus axions at the electro-weak scale do not arise when the two Higgses take a vev.

## 2.3 Stability

We do not address here the question of whether the broken vacuum represents a global minimum of the potential, where, if false, it is necessary to compare the tunneling time for the metastable vacuum with the age of the universe, but rather we ensure it is a local minima by choosing to scan over the physical masses with positive values, whence the local minima conditions of positive eigenvalues of the mass matrix are satisfied automatically. This results from expanding the potential  $V(\psi_i)$  around its extremum  $\psi_i = v_i$ :

$$V(\psi_i) = V(v_i) + \partial_i V(\psi_i - v_i) + \frac{1}{2} (\psi_i - v_i) \partial_{ij} V(\psi_j - v_j), \quad (19)$$

then the tadpole conditions ensures the vanishing of the linear term, whereas the positivity of the matrix  $\partial_{ij}V$  (i.e. the positivity of its eigenvalues) ensures being at a local minimum. The eigenvalues of  $\partial_{ij}V$  are nothing but the “masses” of the fields  $\psi_i$ .

Furthermore, one can impose sufficient conditions for the boundedness of the potential which we do now. We divided the potential into three parts ( $V_{\text{Active}}$ ,  $V_{\text{Inert}}$  and  $V_{\text{Coupled}}$ ), so by requiring each part to be positive, and so bounded from below, we reach sufficient conditions, which may not be necessary ones, for the potential boundedness from below. By Cauchy-Schwartz inequality, we can set for any two complex vectors one angle  $\theta(1, 2)$  and one phase  $\phi(1, 2)$  defined as follows.

$$V_1^\dagger \cdot V_2 = |V_1^\dagger \cdot V_2| e^{i\phi(1,2)} = \|V_1\| \cdot \|V_2\| \cos \theta(1,2) e^{i\phi(1,2)}, \quad \text{where } \theta \in [0, \pi/2], \phi \in [-\pi, \pi] \quad (20)$$

Restricting to fourth order terms, in order to study the large field limit, and assuming all the couplings are real, so  $\xi_{udud} \equiv \xi_{dudu}^* = \xi_{dudu}$

$$V_{\text{Active}} \supseteq \lambda_{uuuu} \|H_u\|^4 + \lambda_{dddd} \|H_d\|^4 + \|H_u\|^2 \|H_d\|^2 (\lambda_{uudd} + \cos^2 \theta(u, d) (\eta_{uddu} + \xi_{udud} \cos 2\phi(u, d))) \quad (21)$$

We know [36] then the following conditions are necessary and sufficient for  $V_{\text{Active}} \geq 0$

$$\lambda_{uuuu} \geq 0, \lambda_{dddd} \geq 0 \quad (22)$$

$$\lambda_{uudd} \geq -2\sqrt{\lambda_{uuuu} \lambda_{dddd}} \quad (23)$$

$$\lambda_{uudd} + \eta_{uddu} \geq |\xi_{udud}| - 2\sqrt{\lambda_{uuuu} \lambda_{dddd}} \quad (24)$$

Now, for the coupled and inert parts of the potential we have, in the large field limit, a generic term of the form  $(\lambda_{a,b,c,d} H_a^\dagger H_b H_c^\dagger H_d)$  where  $a, b, c, d \in \{u, d, 1, 2, 3, 4\}$  with  $\lambda_{a,b,c,d} = \lambda_{c,d,a,b}$  and  $\lambda_{a,b,c,d} \equiv \lambda_{b,a,d,c}^* = \lambda_{b,a,d,c}$ . We see that in order to insure  $(V_{\text{Coupled}} + V_{\text{Inert}})$  is positive, it suffices that any summation of the generic term with the terms corresponding to the permutations over the indices  $(a, b, c, d)$  is positive. More precisely, if we denote the mapping  $\sigma = \begin{pmatrix} 1 & 2 & 3 & 4 \\ a & b & c & d \end{pmatrix}$  then the summand is of the form  $\lambda_{\sigma p(1), \sigma p(2), \sigma p(3), \sigma p(4)} H_{\sigma p(1)}^\dagger H_{\sigma p(2)} H_{\sigma p(3)}^\dagger H_{\sigma p(4)}$  where  $p$  is a permutation in  $S_4$  of 24 elements. Noting that  $\lambda_{a,b,c,d} = \lambda_{c,d,a,b}$ , then  $p$  can span  $S_4/Z_2$  of 12 elements, and using  $\lambda_{a,b,c,d} = \lambda_{b,a,d,c}^*$  one can restrict the sum to six elements forming a set  $\{p_k : k = 1, \dots, 6\}$  corresponding to “independent” couplings<sup>§</sup>, so that we impose

$$\begin{aligned} & \sum_{k=1}^{k=6} 2 \operatorname{Re} \lambda_{\sigma p_k(1), \sigma p_k(2), \sigma p_k(3), \sigma p_k(4)} H_{\sigma p_k(1)}^\dagger H_{\sigma p_k(2)} H_{\sigma p_k(3)}^\dagger H_{\sigma p_k(4)} \\ &= \\ & 2 \|H_a\| \|H_b\| \|H_c\| \|H_d\| \sum_{k=1}^{k=6} \lambda_{\sigma p_k(1), \sigma p_k(2), \sigma p_k(3), \sigma p_k(4)} \cos \theta(\sigma p_k(1), \sigma p_k(2)) \cos \theta(\sigma p_k(3), \sigma p_k(4)) \times \\ & \quad \cos [\phi(\sigma p_k(1), \sigma p_k(2)) + \phi(\sigma p_k(3), \sigma p_k(4))] \\ & \geq 0 \end{aligned} \quad (26)$$

We see that if the independent coupling  $\lambda_{\sigma p_k(1), \sigma p_k(2), \sigma p_k(3), \sigma p_k(4)}$  is switched on, then one can always find a configuration where the phase exists and leads to a blowing downward. Two cases evading this instability happen either when all the indices  $(a, b, c, d)$  are identical leading to  $\theta(a, a) = \phi(a, a) = 0$ , or when they consist of two different indices occurring each twice, such as  $(a, a, b, b)$  or one of its permutations, where we get, noting that  $\theta(a, b) = \theta(b, a)$ ,  $\phi(a, b) = -\phi(b, a)$ , the factor:

$$2 \|H_a\|^2 \|H_b\|^2 [\lambda_{a,a,b,b} + \cos^2 \theta(a, b) (\lambda_{a,b,b,a} + \lambda_{a,b,a,b} \cos 2\phi(a, b))] \quad (27)$$

<sup>§</sup>For example, one can take

$$\begin{aligned} p_1 &= \begin{pmatrix} 1 & 2 & 3 & 4 \\ 1 & 2 & 3 & 4 \end{pmatrix}, p_2 = \begin{pmatrix} 1 & 2 & 3 & 4 \\ 2 & 3 & 4 & 1 \end{pmatrix}, p_3 = \begin{pmatrix} 1 & 2 & 3 & 4 \\ 2 & 1 & 3 & 4 \end{pmatrix} \\ p_4 &= \begin{pmatrix} 1 & 2 & 3 & 4 \\ 1 & 3 & 4 & 2 \end{pmatrix}, p_5 = \begin{pmatrix} 1 & 2 & 3 & 4 \\ 4 & 2 & 3 & 1 \end{pmatrix}, p_6 = \begin{pmatrix} 1 & 2 & 3 & 4 \\ 2 & 3 & 1 & 4 \end{pmatrix} \end{aligned} \quad (25)$$

Applying the above procedure on  $V_{\text{Active}}$  (Eq. 16) we get the following sufficient conditions for its positivity in the large field limit. ( $I \in \{u, d\}, \alpha \in \{1, 2, 3, 4\}$ )

$$\begin{aligned}
\lambda_{II\alpha\beta} &= \eta_{I\alpha\beta I} = \xi_{I\alpha I\beta} = 0, \quad \text{for } \alpha < \beta \\
\lambda_{II\alpha\alpha} &\geq 0, \\
\lambda_{II\alpha\alpha} + \eta_{I\alpha\alpha I} &\geq |\xi_{I\alpha I\alpha}| \\
&\Rightarrow \\
V_{\text{Coupled}} &\geq 0
\end{aligned} \tag{28}$$

Note that here we did not get a relation relating, say,  $\lambda_{I,I,\alpha,\alpha}$  with  $\lambda_{I,I,I,I}$ , because the term corresponding to the latter ( $\lambda_{I,I,I,I} \|H_I\|^4$ ) has already been considered in deriving Eqs. (23, 24).

Applying similarly the procedure on  $V_{\text{Inert}}$  (Eq. 15), we get the following sufficient conditions for its stability

$$\begin{aligned}
\lambda_{\alpha\alpha\alpha\alpha} &\geq 0, \\
\lambda_{\alpha\alpha\alpha\beta} &= 0, \quad \text{for } \alpha < \beta, \\
\lambda_{\alpha\alpha\beta\gamma} &= \lambda_{\alpha\beta\gamma\alpha} = \lambda_{\gamma\alpha\beta\alpha} = 0, \quad \text{for } \alpha < \beta < \gamma, \\
\lambda_{\alpha\beta\gamma\delta} &= \lambda_{\beta\gamma\delta\alpha} = \lambda_{\beta\alpha\gamma\delta} = \lambda_{\alpha\gamma\delta\beta} = \lambda_{\delta\beta\gamma\alpha} = \lambda_{\beta\gamma\alpha\delta} = 0, \quad \text{for } \alpha < \beta < \gamma < \delta, \\
\lambda_{\alpha\alpha\beta\beta} &\geq 0, \quad \text{for } \alpha < \beta, \\
\lambda_{\alpha\alpha\beta\beta} + \lambda_{\alpha\beta\beta\alpha} &\geq |2\lambda_{\alpha\beta\alpha\beta}|, \quad \text{for } \alpha < \beta, \\
&\Rightarrow \\
V_{\text{Inert}} &\geq 0
\end{aligned} \tag{29}$$

Note again that we did not seek to find a relation, as in Eqs. (23, 24), relating, say,  $\lambda_{\alpha\alpha\beta\beta}$  with  $\lambda_{\alpha\alpha\alpha\alpha}$ , because if we impose the copositivity of the sum of terms corresponding to these two couplings ( $\lambda_{\alpha\alpha\alpha\alpha} \|H_a\|^4 + \lambda_{\beta\beta\beta\beta} \|H_\beta\|^4 + \lambda_{\alpha\alpha\beta\beta} \|H_\alpha\|^2 \|H_\beta\|^2$ , for  $\cos\theta(\alpha, \beta) = 0$ ), then we can no longer use the term ( $\lambda_{\alpha\alpha\alpha\alpha} \|H_\alpha\|^4$ ) to find a relation relating it to  $\lambda_{\alpha\alpha\gamma\gamma}$  with  $\gamma \neq \beta$ .

To summarize, if we take the conditions of Eqs. (22, 23, 24, 28 and 29) then we guarantee that the potential is positive in the large field limit, and thus is bounded from below.

## 2.4 Active Sector

The mass spectrum in 2HDM has been given in some papers [37]. We denote the two Higgses as follows.

$$H_u = \begin{pmatrix} H_u^+ \\ \phi_u + v_u + i\sigma_u \end{pmatrix}, \quad H_d = \begin{pmatrix} H_d^+ \\ \phi_d + v_d + i\sigma_d \end{pmatrix} \tag{30}$$

The neutral CP-even fields ( $\phi_u, \phi_d$ ) mix through a rotation matrix  $Z^H$ , characterized by an angle  $\alpha$ , to give mass eigenstates ( $h_1, h_2$ ). The neutral CP-odd fields ( $\sigma_u, \sigma_d$ ) equally mix through a rotation matrix  $Z^A$  characterized by an angle  $\beta$  to give mass eigenfields ( $A_1^0, A_2^0$ ) where  $A_1^0$  is a massless Goldstone boson. Finally, the charged fields ( $H_u^+, H_d^+$ ) will mix through a rotation matrix  $Z^+$  characterized, up to a sign, by the same angle  $\beta$  to give mass eigenstates ( $H_1^+, H_2^+$ ) with massless Goldstone  $H_1^+$ . Thus we have five physical Higgses from the two doublets  $H_u, H_d$ : 2 CP-even neutral ( $h_1, h_2$ ) with respective masses ( $M_H = 125 \text{ GeV}, M_e$ ), 1 CP-odd neutral ( $A_2^0$ ) with mass  $M_o$  and 2 charged Higgses ( $H_2^+, H_2^-$ ) with mass  $M_c$ .

We have seven free coupling parameters ( $\mu_u^2, \mu_d^2, \lambda_{uuuu}, \lambda_{dddd}, \lambda_{uudd}, \eta_{uudd}, \xi_{uud}$ ). We have also two vevs  $v_u, v_d$  with  $v_u^2 + v_d^2 = v_{\text{SM}}^2 = 246^2 \text{ GeV}^2$ , determined by imposing the two tadpole conditions  $\partial_{\phi_u} V_{\text{Active}}|_{\phi_u=v_u, \phi_d=v_d} = 0, \partial_{\phi_d} V_{\text{Active}}|_{\phi_u=v_u, \phi_d=v_d} = 0$ . We define  $\tan\beta = \frac{v_d}{v_u}$ .

We shall tradeoff our free parameters with the following physical parameters: ( $M_H = 125, M_e, M_o, M_c, \alpha, v = v_{\text{SM}}, \tan\beta$ ).

In Appendix (B.2.1), we state all the related formulae in the enumerations (1, 2, 3).

## 2.5 Inert Sector

We denote the additional Higgs doublets ( $\alpha = 1, 2, 3, 4$ ) by:

$$H_\alpha = \begin{pmatrix} H_\alpha^+ \\ \phi_\alpha + i\sigma_\alpha \end{pmatrix} \quad (31)$$

Again, the neutral CP-even (odd) fields  $\phi_\alpha$  ( $\sigma_\alpha$ ) mix amidst themselves with rotation matrix  $ZH^i$  ( $ZA^i$ ). Equally, the charged fields  $H_\alpha^+$  mix together with rotation matrix  $ZP^i$

In Appendix (B.2.1), we state all the related formulae in the enumerations (4, 5, 6). The scalar particle content appears in Table form in Appendix (B.3).

## 3 “Symmetric” Benchmark Point

In some regions of the 2HDM parameter space there is a decoupling limit in which the masses of the CP-odd and charged fields are quite larger than those of two CP-even. Because our purpose is to see whether or not the (LAH) in our model can be a component of the DM, we limit ourselves for simplicity to this decoupling limit, as we shall now explain. Also, for the “Inert” section we opt for a simplifying choice which amounts to decouple one “light” doublet (say the 1st) from the other “heavy” doublets, as will become clearer shortly. The benchmark point we end up resembles thus a special (2+1) model which is worthy to be investigated on its own merit.

### 3.1 Active Sector Benchmark Point

We fix our parameter space at an experimentally accepted point known as the “Alignment Limit” satisfying  $(\sin(\beta - \alpha) = 1)$  [27].

Furthermore, we go for a “symmetric” alignment limit in the sense we take:

$$\alpha = -\beta = -\pi/4 \Rightarrow \tan \beta = 1 \quad (32)$$

We note that the choice  $\alpha = 0$  is rejected by the current data [27]. Finally, we decouple the CP-odd and charged Higgses from the CP-even Higgs, and take a “democratic” limit, acceptable according to [27], reducing the parameters number and mimicking the IDM:

$$M_{h_1} = M_{h_2} \equiv M_H = 125 \text{ GeV} , \quad M_o, M_c \gg 125 \text{ GeV} \quad (33)$$

In fact, there is a limit in the 2HDM parameter space corresponding to degenerate CP-even Higgs fields decoupled from heavy CP-odd and charged Higgses, which was, together with other decoupling degenerate points, thoroughly studied in [38] and contrasted to the LHC data. To see this, it suffices to “fine tune” and take the following constraints on the lagrangian parameters:

$$\begin{aligned} \left| \frac{\lambda_{uuuu}}{\xi_{udud}} \right| &= \mathcal{O}(\epsilon) \quad , \quad \left| \frac{\lambda_{uuuu}}{\xi_{udud} + \eta_{uddu}} \right| = \mathcal{O}(\epsilon), \\ \left| \frac{\xi_{udud} + \eta_{uddu} + \lambda_{uudd}}{\lambda_{uuuu}} \right| &= \left| \mathcal{O}\left(\frac{1}{\epsilon}\right) + \frac{\lambda_{uudd}}{\lambda_{uuuu}} \right| = \mathcal{O}(\epsilon) \quad , \quad \left| \frac{\lambda_{uuuu} - \lambda_{dddd}}{\lambda_{uuuu}} \right| = \left| 1 - \frac{\lambda_{dddd}}{\lambda_{uuuu}} \right| = \mathcal{O}(\epsilon^2) \end{aligned} \quad (34)$$

with  $\epsilon \ll 1$ , then with the choice  $\tan \beta = 1$  we see from Eq. (65, 69, 71) that  $M_0, M_c \gg M_{h_1} \approx M_{h_2}$  and that  $|\alpha| = |\beta| = \pi/4$ .<sup>¶</sup> Note here that it is the combination  $(\xi_{udud} + \eta_{uddu} + \lambda_{uudd})$  which enters as a perturbative parameter in the unitarity constraints. Note also that  $M_o, M_c$ , albeit being large, should not be too heavy in a way to affect the gauge couplings unification.

<sup>¶</sup>We shall state our results to zeroth order in  $\epsilon$

### 3.2 Inert Sector Benchmark Point

We set now our benchmark point in the “inert” sector with many simplifying assumptions. As we shall see, these “strong” assumptions lead to singling out the LAH easily, and to decouple it from the rest of the spectrum. Our objective is to reduce the number of parameters, and see whether or not the recovered LAH can account for DM.

First, we assume all the off-diagonal elements of the mass matrices for CP-even (odd) and charged Higgs fields (Eqs. 72, 73 and 74) are zero. Thus, we have:

$$m_F^2 = \text{diag}(M_{11}^F, M_{22}^F, M_{33}^F, M_{44}^F), \quad (35)$$

where  $F \in \{h^i, A^{i0}, H^{i+}\}$ . Second, we assume that only the first inert doublet is coupled to the active sector, i.e.

$$\text{For } I = u, d, \alpha = 2, 3, 4 \quad , \quad \lambda_{II\alpha\alpha} = \eta_{I\alpha\alpha I} = \xi_{I\alpha I\alpha} = 0. \quad (36)$$

Looking again at Eqs (72, 73 and 74) we have then

$$M_{\alpha\alpha}^F = \mu_{\alpha\alpha}, \alpha = 2, 3, 4 \quad (37)$$

and

$$M_{e1}^2 \equiv M_{11}^{h^i} = \mu_{11} + (\lambda_{uu11} + \eta_{u11u} + \xi_{u1u1})v_u^2 + (\lambda_{dd11} + \eta_{d11d} + \xi_{d1d1})v_d^2, \quad (38)$$

$$M_{o1}^2 \equiv M_{11}^{A^{i0}} = \mu_{11} + (\lambda_{uu11} + \eta_{u11u} - \xi_{u1u1})v_u^2 + (\lambda_{dd11} + \eta_{d11d} - \xi_{d1d1})v_d^2, \quad (39)$$

$$M_{c1}^2 \equiv M_{11}^{H^{i+}} = \mu_{11} + (\lambda_{uu11})v_u^2 + (\lambda_{dd11})v_d^2, \quad (40)$$

Third, we assume that  $\phi_1$  decouples from  $\phi_\alpha$  for  $\alpha = 2, 3, 4$ , by imposing

$$\mu_{\alpha\alpha}/\mu_{11} \gg 1, \alpha = 2, 3, 4 \quad (41)$$

As to  $M_{11}^F$  (Eqs. 38, 39 and 40), we see that we have seven parameters. Fourth, we impose an u-d symmetric condition:

$$\lambda_{uu11} = \lambda_{dd11}, \eta_{u11u} = \eta_{d11d} \quad \text{and} \quad \xi_{u1u1} = \xi_{d1d1} \quad (42)$$

Thus we end up with four parameters which determine the elements  $M_{11}^F$ . If we denote now

$$\lambda = \lambda_1 \equiv \lambda_{uu11} + \eta_{u11u} + \xi_{u1u1} = \lambda_2 \equiv \lambda_{dd11} + \eta_{d11d} + \xi_{d1d1}, \quad (43)$$

then we can tradeoff the four free parameters by the masses  $M_{e1}, M_{o1}, M_{c1}$  and the constant  $\lambda$  expressing the coupling strength between the DM and the active Higgs field. Finally, and as a fifth assumption similar to our assumption in the 2HDM, we decouple CP-even inert Higgs from the CP-odd and charged inert Higgses by assuming:

$$M_{o1}, M_{c1} \gg M_{e1} \quad (44)$$

Looking at Eqs. (38, 39 and 40), we see that this assumption means restricting ourselves to a region in the parameter space where  $|\lambda/(\lambda + \eta + \xi)| \gg 1, |(\lambda + \eta - \xi)/(\lambda + \eta + \xi)| \gg 1$  but  $|\lambda + \eta + \xi|$  is finite. Note again that it is the combination  $(\lambda + \eta + \xi)$  which is involved in the vertex between physical states and which should be perturbative in order to respect the constraints of unitarity.

We call the point which satisfies the above five assumptions in the inert sector by the “Symmetric Dark” benchmark, as it corresponds to symmetric couplings of  $H_u$  and  $H_d$  to the remaining light inert doublet containing our DM candidate. At the “symmetric dark” benchmark, the free parameters of the dark sector are determined only by two free parameters  $M_{e1} \equiv M_{DM}, \lambda$ , putting aside the self-coupling  $\lambda_{1111}$ . Now the LAH, referred to by  $\psi$  is nothing but the lightest neutral component of the inert doublet  $h_1^i$ . The simplicity of the “Symmetric Dark” benchmark point and the reduced number of its free parameters to be scanned is what pushed us to consider it for the sake of demonstrating the model viability.

### 3.3 Total Benchmark Point

Our “symmetric choice” benchmark is the the “symmetric alignment limit” of the active sector ( $v_u = v_d$ ) PLUS the “symmetric Dark” benchmark point. Thus we have

$$M_{DM}^2 = M_{e1}^2 = M_\psi^2 = \mu_{11} + \lambda v^2 \quad (45)$$

The last column of the Table in Appendix (B.3) shows the mass decoupling at the “Symmetric choice” benchmark  $\parallel$ .

Although our chosen point in (2+4) scenario can not be distinguished, as long as dark matter is concerned, from the (2+1) scenario, nonetheless, we need six Higgs doublets for unification purposes.

## 4 Phenomenology

As said earlier, we restricted the phenomenological analysis to our “symmetric choice” benchmark point, as the stress in this work is on model building and its viability for accommodating DM. However, this benchmark is important in itself, as it represents a special case of the (2+1) model when  $M_{h_1} = M_{h_2}$ . However, it is not equivalent to the IDM, as the active Higgses can be differentiated by their decay products and can not be identified both to the LHC Higgs, in that  $h_1$  can not decay directly to gauge bosons in contrast to  $h_2$ .

We used for the numerics the Mathematica packages (*Sarah* + *FeynArts* + *FormCalc*), where we computed explicitly all the relevant quantities, with no need to go to some “blackbox” packages, such as micrOMEGAs. We made use, however, of the latter package in order to check consistency with mathematica results concerning the different adopted constraints.

### 4.1 Relic Density

An appealing aspect of WIMPs as DM candidate is that it could be produced naturally with an abundance of approximately the correct order of magnitude [39]. By using the current observational data on DM abundance, further constraints on the parameter space can be obtained.

If we assume that the DM is produced in a thermal process, and the production process ceases before annihilation, then its abundance evolves as

$$\frac{dn_\psi}{dt} = -3Hn_\psi - \langle \sigma_{\text{tot}} v_{\text{rel}} \rangle (n_\psi^2 - (n_\psi^{\text{eq}})^2). \quad (46)$$

where  $H$  is the Hubble parameter,  $n_\psi^{\text{eq}}$  is the equilibrium density of the particle  $\psi$ , and  $\langle \sigma_{\text{tot}} v_{\text{rel}} \rangle$  is the thermal average of the annihilation cross section. The DM abundance freezes as annihilation rate drops below the Hubble rate, and if we denote  $Y_\infty$  as the asymptotic ratio of DM number density to entropy density, then upon expanding the cross section to first order in powers of  $x^{-1} \equiv \frac{T}{m_\psi}$ , so that to write  $\langle \sigma_{\text{tot}} v_{\text{rel}} \rangle = \sigma_0(1 + b x^{-1})$ , then  $Y_\infty$  is given by [30]

$$Y_\infty = \frac{n_{\psi0}}{s_0} = \frac{3.79x_f}{\left(\frac{g_{*S}}{\sqrt{g_*}}\right)m_{PL}m_\psi\sigma_0(1 + \frac{b}{2x_f})} \quad (47)$$

with

$$x_f = \log \left[ 0.038 \frac{g_\psi}{\sqrt{g_*}} m_{pl} m_\psi \sigma_0 \right] - \frac{1}{2} \log \left[ \log \left[ 0.038 \frac{g_\psi}{\sqrt{g_*}} m_{pl} m_\psi \sigma_0 \right] \right] + \log \left[ 1 + \frac{b}{\log \left[ 0.038 \frac{g_\psi}{\sqrt{g_*}} m_{pl} m_\psi \sigma_0 \right]} \right] \quad (48)$$

where  $g_\psi = 1$  for the scalar boson  $\psi$ . As to  $g_*$ , it counts the total number of effectively mass degrees of freedom (for species with mass far less than the temperature), whereas  $g_{*S}$  expresses a proportionality

---

$\parallel$ Upon request, we can provide the Feynman rules for the vertices at the chosen benchmark point.

between the entropy density and  $T^3$ , and for all particle species, except neutrino, can be replaced by  $g_*$  for most of the history of universe. Thus, we get finally [30]:

$$\Omega_\psi \equiv \frac{n_\psi m_\psi}{\rho_c} \implies \Omega h^2 = \frac{1.07 \times 10^9 x_f \text{ GeV}}{\sqrt{g_*} m_{pl} \sigma_0 \left(1 + \frac{b}{2x_f}\right)} \quad (49)$$

With our model we may calculate explicitly the annihilation cross section of  $\psi$ . We shall include only tree diagrams, and consider only annihilations involving 2-body final states, as final states involving three bodies or more are suppressed by the phase space factor. The Feynman diagrams responsible for such interaction can be classified into two categories: the first involves 4-point vertices leading to gauge bosons or 2HDM Higgses, and the second has an s-channel for an intermediate Higgs ( $h_1$  or  $h_2$ ) or a t(u)-channel with an intermediate  $\psi$ . At the tree level, the annihilation can not proceed via intermediate gauge bosons because of the absence of  $\psi\psi W(Z)$  vertices. For completeness, we state in Appendix C all the annihilation amplitudes where we used the FaynArts, FormCalc packages in order to compute the polarization sum for bosons, and the helicity/color sum for fermions.

We have used the method of [41, 40, 31] for taking the thermal average. Precisely, we use the following formulae for the thermal average of annihilation of initial two bodies with masses  $m_1, m_2$ :

$$\langle \sigma v_{rel} \rangle = \frac{1}{m_1 m_2} \left(1 - \frac{3(m_1 + m_2)T}{2m_1 m_2}\right) w(s) \quad (50)$$

where:

$$w(s) = \frac{1}{32\pi} \frac{p_f(s)}{s^{1/2}} \int_{-1}^{+1} d \cos \theta_{CM} |\mathcal{M}|^2 \quad (51)$$

$$s = (m_1 + m_2)^2 + 3(m_1 + m_2)T \quad (52)$$

where  $p_f(s)$  is the magnitude of the three-momentum of one of the final particles in the center-of-mass frame.

We determine the freezing temperature  $T_f$  by iteration. For a given  $T$ , we compute the thermal average  $\langle \sigma v_{rel} \rangle$  using Eqs. (50, 51), which we expand in powers of  $T$  to determine the coefficients  $\sigma_0, b$ . We compute  $g_*(T)$  using the formula [30]:

$$g_* = \sum_{i=\text{boson}} g_i + \frac{7}{8} \sum_{i=\text{fermion}} g_i \quad (53)$$

where  $g_i$  expresses the number of internal degrees of freedom of the species  $i$  with mass  $m_i$  less than the temperature  $T$ , then we compute the “new” temperature using Eq. (48). We iterate till we get convergence.

We note also that in order to determine the coefficients of the expansion  $\langle \sigma v_{rel} \rangle(T) = \sum_n (\text{coef.})_n T^n$ , the function  $\langle \sigma v_{rel} \rangle(T)$  is not a continuous function. Thus, we can not by simple differentiation determine the linear term. What we did is to find the best fit of a linear term by using the method of Least Square Error in the range  $T \leq T_f$  since the thermal average formulae are valid only for this range [31].

We draw the attention that in our explicit analysis, one should not expect a complete agreement with the more sophisticated packages like micrOMEGAs. In fact, we know [42] that expanding the thermal average  $\langle \sigma v_{rel} \rangle_T = \sum_n (\text{coef.})_n T^n$  is not valid at resonances and/or at thresholds, and one should take account of many effects including, say, the Sommerfeld enhancement. For the resonance in our case, we have the kinematically allowed limit  $M_\psi = \frac{1}{2} M_H$  and our resonance is limited to Higgs, since DM can only annihilate via Higgs. Equally, one should amend the formula around the thresholds  $s = 4M_f^2$  for a final product of mass  $M_f$ . However we checked partially when comparing to micrOMEGAs that the effects due to these changes are small and do not change much the phenomenology. Actually, the micrOMEGAs package uses corrected formulae, and although our initial analysis may give different results around resonances and thresholds, but we checked locally around many chosen points at this critical region that discrepancies are numerically small. Since, in our scan, we took  $M_\psi > 2M_q$  for all light quarks, so the first threshold effect should appear at the masses of the  $Z, W^+$  gauge bosons.

Moreover, in our analysis, there is no role for co-annihilation, as there is no particle in the dark sector with mass close to  $M_{DM}$  in our chosen “symmetric” benchmark point.

Phenomenologically, we did not equate the DM relic density to a given value and solved, at fixed  $M_{DM}$  ( $\lambda$ ), for  $\lambda$  ( $M_{DM}$ ). Rather, we fixed  $M_{DM}$  ( $\lambda$ ), and plotted the DM relic density as a function of  $\lambda$  ( $M_{DM}$ ). We can now determine and visualize the accepted region of  $\lambda$  ( $M_{DM}$ ) for the taken fixed value of  $M_{DM}$  ( $\lambda$ ) by imposing a band condition on the DM relic density. In fact we have scanned a 2-dim parameter space of  $\lambda$  and  $M_{DM}$ , spanning 300000 points on a simple core i5 intel processor, and for each parameter space point we imposed the band condition.

In Fig. 2(3),  $\Omega$  is plotted versus  $M_\psi$  ( $\lambda$ ) for 5 fixed values of  $\lambda$  ( $M_\psi$ ).

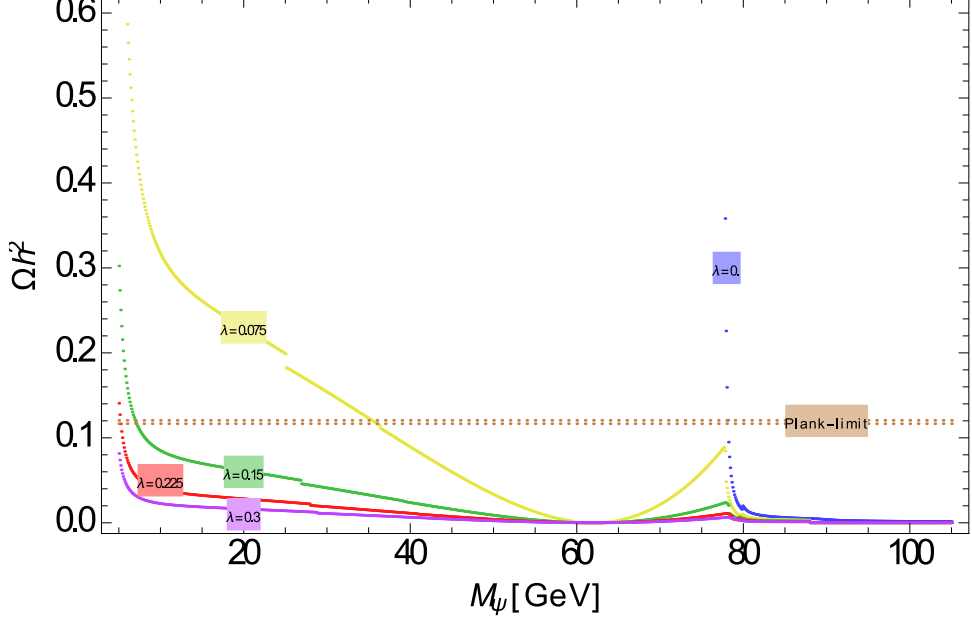


Figure 2: Relic Density versus  $M_\psi$  for 5 fixed values of  $\lambda$ . “Acceptable” Planck limits are also shown.

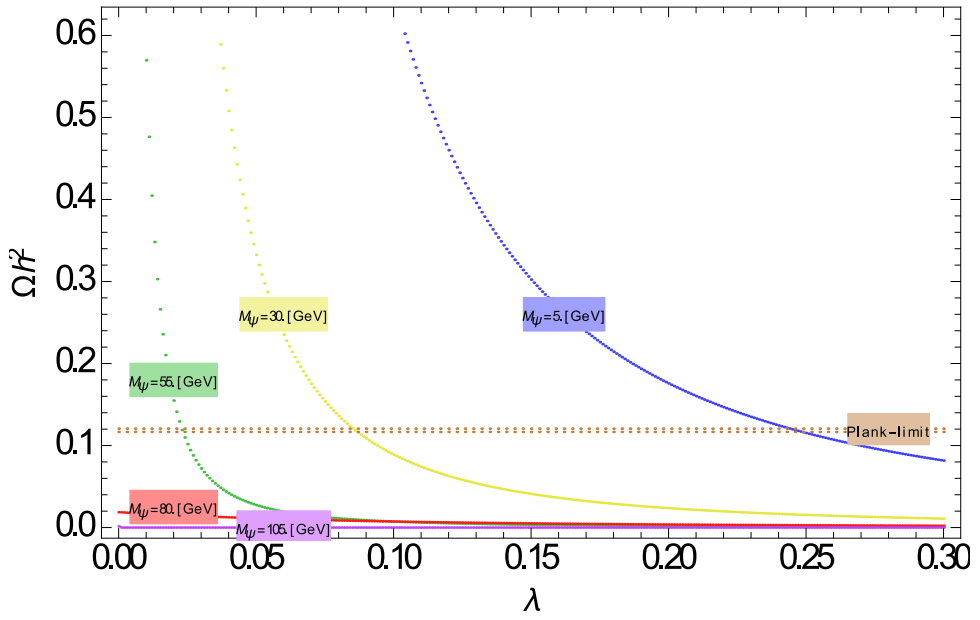


Figure 3: Relic Density versus  $\lambda$  for 5 fixed values of  $M_\psi$ . “Acceptable” Planck limits are also shown.

## 4.2 Direct Detection

The connection between  $\lambda$  and  $m_\psi$  derived from the abundance constraint is very predictive. It has consequences for current DM searches. The sensitivity of DM detectors to  $\psi$  particles is controlled by their elastic scattering cross section with visible matter, and in particular with nuclei. In fact, this cross section is the relevant quantity to be measured in the current experiments designed to measure the recoil signal of DM collisions within detectors [43, 44]. More specifically, we shall state the Direct Detection (DD) constraints at the level of scattering off nucleons. Actually, there are well known formulae starting from the nucleon's ones in order to compute the DD cross section between DM and nuclei [46].

Also, the elastic DM-nucleon scattering controls the abundance of DM particles trapped at the terrestrial or solar core, and whose presence is detected indirectly through the flux of energetic neutrinos which is produced by subsequent DM annihilations. However, in this work, we shall not pursue the viability of the model with respect to indirect detection.

The Feynman diagram describing elastic  $\psi$ -particle collisions with nucleons corresponds to a T-channel via an intermediate 2HDM Higgs  $h_1, h_2$ . We assume loop diagrams exchanging gauge bosons to be neglected because of the presence of more than one propagator, contrary to tree-level diagrams.

We use the non-relativistic approximation for the incoming particles, and thus apply low energy theorems to have an effective Higgs-Nucleon coupling [47]

$$\eta_N \equiv g_{HNN} \approx \frac{gM_N}{2M_W} \frac{2N_H}{3q} \quad (54)$$

where  $M_N \approx 939\text{MeV}$  is the nucleon mass,  $N_H$  is the number of heavy quarks whose masses exceed the Higgs mass and  $q = 11 - \frac{2}{3}n_L$  with  $n_L = 6 - N_H$  the number of light quarks. We get in Appendix (D) a scattering amplitude given by Eq. (83) and a thermal average for the elastic  $\psi - N$  scattering given by Eq. (84).

The LUX experiment [43] puts an upper bound  $2.2 \times 10^{-46} \text{ cm}^2$  on  $\langle \sigma_{\text{el}} v \rangle$ , whereas the Xenon100 experiment [44] puts a larger upper bound ( $1.1 \times 10^{-45} \text{ cm}^2$ ).

In Fig. 4, we plot  $\sigma_{\text{el}}$  versus  $M_\psi$  for a fixed value of  $\lambda$ , and we show the LUX limit on the figure showing that for various decreasing values of  $\lambda$  considerable augmenting ranges of  $M_\psi$  pass the DD constraint. In contrast, in Fig. 5 we plot  $\sigma_{\text{el}}$  versus  $\lambda$  for five fixed value of  $M_\psi$ , and we see that the acceptable range of  $\lambda$  shrinks as  $M_\psi$  decreases.

When we scan the 2-dim parameter space of  $(M_\psi, \lambda)$  we see that LUX experiment allows just a small region around resonance (DM is light around 62 GeV), whereas for Xenon100 there is a much larger portion which is not excluded. \*\*

## 4.3 Invisible Higgs Decay

As said earlier, one can distinguish  $h_1$  from  $h_2$  by their decay products. ††. The Higgs  $h_2$  can decay via 4 channels  $\psi\psi, f\bar{f}, W^+W^-$  and  $Z, Z$  whereas the Higgs  $h_1$  decays only to  $f\bar{f}$ . We identify the LHC Higgs by  $h_2$  and take the Invisible Higgs Decay (IHD) constraint to be:

$$\left| \frac{h_2 \rightarrow DM + DM}{h_2 \rightarrow X} \right|^2 < 0.2 \quad (55)$$

For completeness, we list in Appendix E all the IHD amplitudes.

In Figs. (6, 7), we show respectively the IHD ratio vs  $(m_\psi, \lambda)$  showing acceptable points with respect to the IHD constraint.

---

\*\*One should note however that the approximation of Eq. (54) is a crude one, and, in a more refined analysis, tougher exclusion curves, resulting from the experimental data, are expected. However, the study of [45] argued that the interplay of annihilation, co-annihilation and semi-annihilation processes relax the DD constraints in various non-minimal scalar Higgs portal DM models.

†† $h_u, h_d$  become  $h_1, h_2$  mass Eigenstates. In our benchmark  $M_{h_1} = M_{h_2} = M_{\text{higgs}}$ . However, the vertex  $(h_2, \psi, \psi) \neq 0$  whereas the vertex  $(h_1, \psi, \psi) = 0$ .

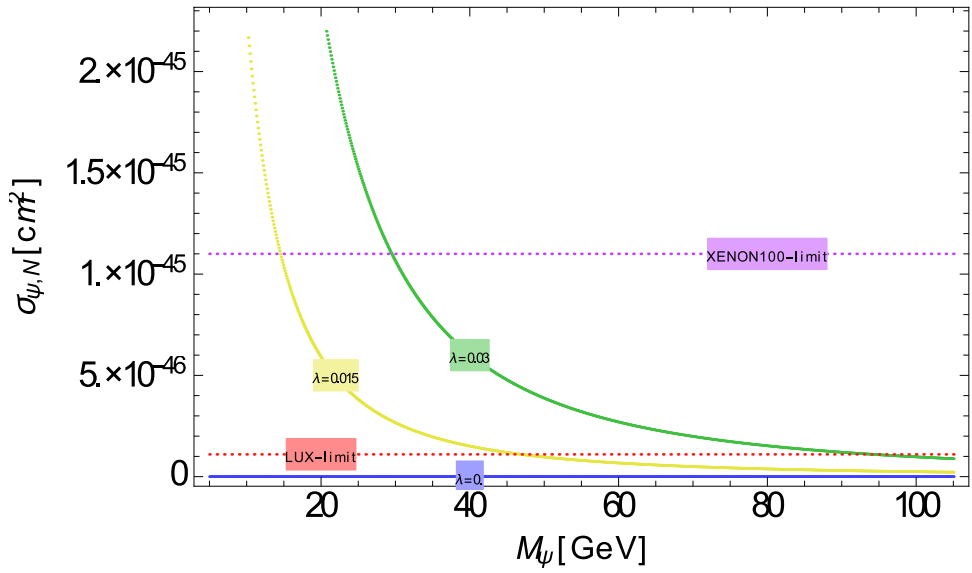


Figure 4: Direct Detection: Nucleon- $\psi$  scattering amplitude versus  $M_\psi$  for 3 fixed values of  $\lambda$ . LUX and Xenon100 limits, above which lie excluded regions, are also shown.

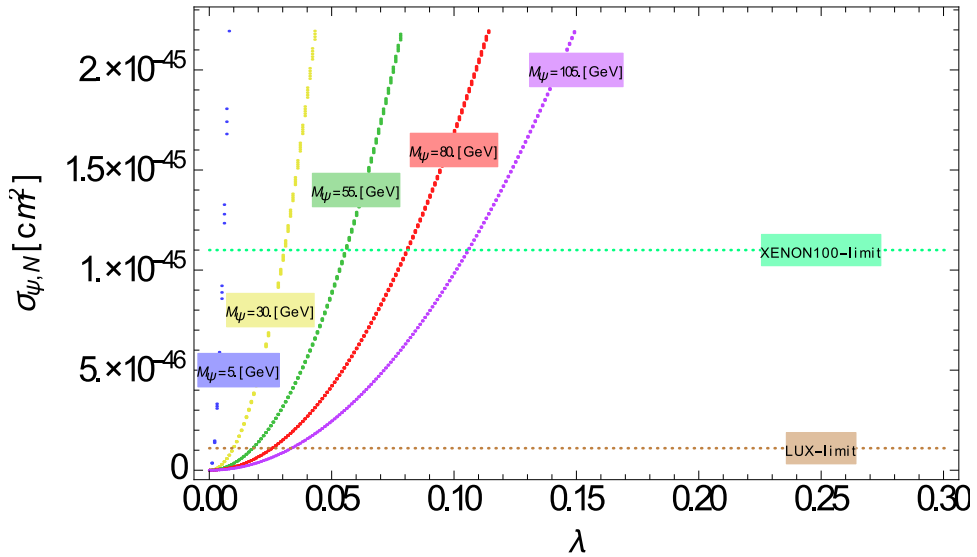


Figure 5: Direct Detection: Nucleon- $\psi$  scattering amplitude versus  $\lambda$  for 5 fixed values of  $M_\psi$ . LUX and Xenon100 limits, above which lie excluded regions, are also shown.

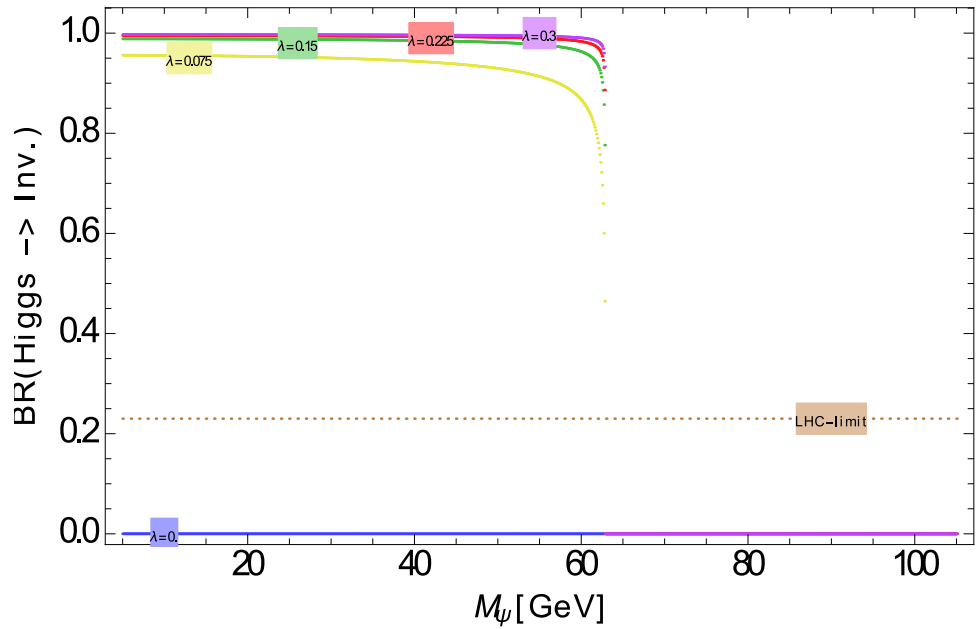


Figure 6: Branching Ratio of Invisible Higgs Decay versus  $M_\psi$  for 5 fixed values of  $\lambda$ . The LHC limit, above which is an excluded region, is also shown.

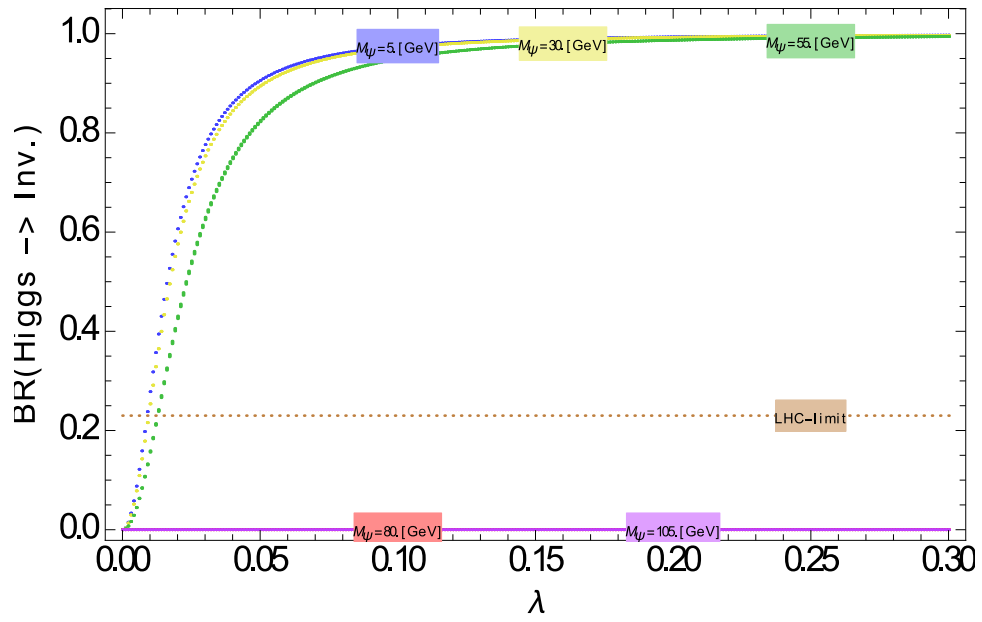


Figure 7: Branching Ratio of Invisible Higgs Decay versus  $\lambda$  for 5 fixed values of  $M_\psi$ . The LHC limit, above which is an excluded region, is also shown.

#### 4.4 Mean Free Path

We estimate here the mean free path  $l_\psi$  of the DM, which should be larger than 1 kpc, otherwise DM particles would behave as a collisional gas altering substantially the halo structure and evolution. We have:

$$l_\psi = \frac{1}{\sigma_{\psi\psi} n_\psi} = \frac{m_\psi}{\sigma_{\psi\psi} \rho_\psi^h} , \quad (56)$$

where  $n_\psi$  and  $\rho_\psi^h$  are the number and mass density in the halo of the  $\psi$  particle, respectively, and we use  $\rho_\psi^h \approx 0.4 \text{ GeV/cm}^3$ , corresponding to the halo density.

The amplitude of the elastic  $\psi - \psi$  scattering is stated in Appendix F (Eq. (89))<sup>‡‡</sup>. We note that it is only here where the “self”-coupling ( $\lambda_S \equiv \lambda_{1111}$ ) interferes. Using  $t = -2(1 - \cos\theta)(\frac{s}{4} - m_\psi^2)$ ,  $u = -2(1 + \cos\theta)(\frac{s}{4} - m_\psi^2)$  with  $\theta$  is the scattering angle in the center of mass frame, we get Eq. (90), in Appendix F, expressing the thermal average of the self-elastic scattering cross section  $\langle \sigma_{\text{el}} \rangle$ .

We can plug in values for  $m_\psi, \lambda$  corresponding to points which have passed the constraints of relic density, DD and IHD, and compute  $\sigma_{\text{el}}$  and  $l_\psi$  for some choices of the DM self-coupling  $\lambda_S$ , which is completely unconstrained by the relic abundance condition.

For a “generic” choice of parameters, with a ‘perturbative’ value for  $\lambda_S$ , we typically get a mean free path of the order of  $10^7 \text{ Mpc}$  or larger, similar to other CDM candidates. It is well known that the CDM model has the so called “missing satellite” problem [48], though its solution may either originate from the distinctive property of the dark matter particles (e.g. warm dark matter or strongly self-interacting dark matter), or be due to astrophysical reasons such as negative feedback of star formation in the small subhalos. We note that while the generic 6HDM model is in this respect similar to other CDM models, the model in special circumstances may provide some mechanism to help solve this problem, e.g. the mean free path may be shortened (look at Eq. 90) with a very large self coupling  $\lambda_S$ , or pushing down the mass of  $\psi$  to the Mev range. Also, we have considered here  $\psi$  as the dominant contribution to DM, but there may be scenarios where it is only part of the DM, which could open ways to solve this galactic-scale problem.

### 5 Conclusions

Fig. 8 represents the phenomenological analysis of the (2+4) model at the “symmetric choice” benchmark point. The two axes represent our 2-dim parameter space spanned by  $(m_\psi, \lambda)$ , where  $\lambda$  is restricted to be “perturbative” ( $\lambda \leq 1$ ). The “black” band represent the points which satisfy the RD constraint [49]:

$$\Omega h^2 \in 0.1186 \pm 0.0020 \quad (57)$$

Although we scanned  $m_\psi$  in the range [5 GeV, 1 TeV], we could only find points satisfying the RD constraint in the range  $m_\psi < 100 \text{ GeV}$ , to which we restricted the horizontal axis in Fig. 8.

The “red” line represents the DD LUX limit, above which is to be excluded. We also state the DD Xenon100 limit (“green” line) which excludes less regions than the LUX limit. The “blue” line represents the IHD constraint keeping the region underneath. We see that there is a viable region in parameter space around the resonance ( $m_H/2$ ) satisfying all the constraints.

Looking at the black relic density band, we see two decreases around the resonance ( $m_H/2$ ) and the threshold ( $m_Z \simeq m_W$ ). This is to be expected as, in general terms, one expects that the annihilation cross section would increase around the resonance. In order to get non-negligible DM relic density, we need thus to decrease the coupling  $\lambda$  around the resonance. Similarly, and because of the channel  $DM+DM \rightarrow WW$ , we expect a decrease in  $\lambda$  when  $M_{\text{DM}}$  is around  $M_W$ . In our “symmetric” benchmark

<sup>‡‡</sup>Loop diagrams involving gauge bosons are dropped numerically. This comes because a such diagram would be accounted for by a renormalized self-coupling  $\lambda_S^R$  and a logarithmic term. The latter, on dimensional grounds, would be proportional to  $g^4 \ln \frac{s}{m_W^2}$  to be compared with the intermediate Higgs s-channel diagram which is proportional to  $\lambda^2 \frac{m_W^2}{m_H^2}$ , with the total energy-squared  $s$  proportional to  $m_\psi^2$ . One can see now that, since  $m_\psi^2, m_W^2, m_H^2$  fall all in the weak scale, there are numerical choices making the logarithmic term far less than the tree-level corresponding term.

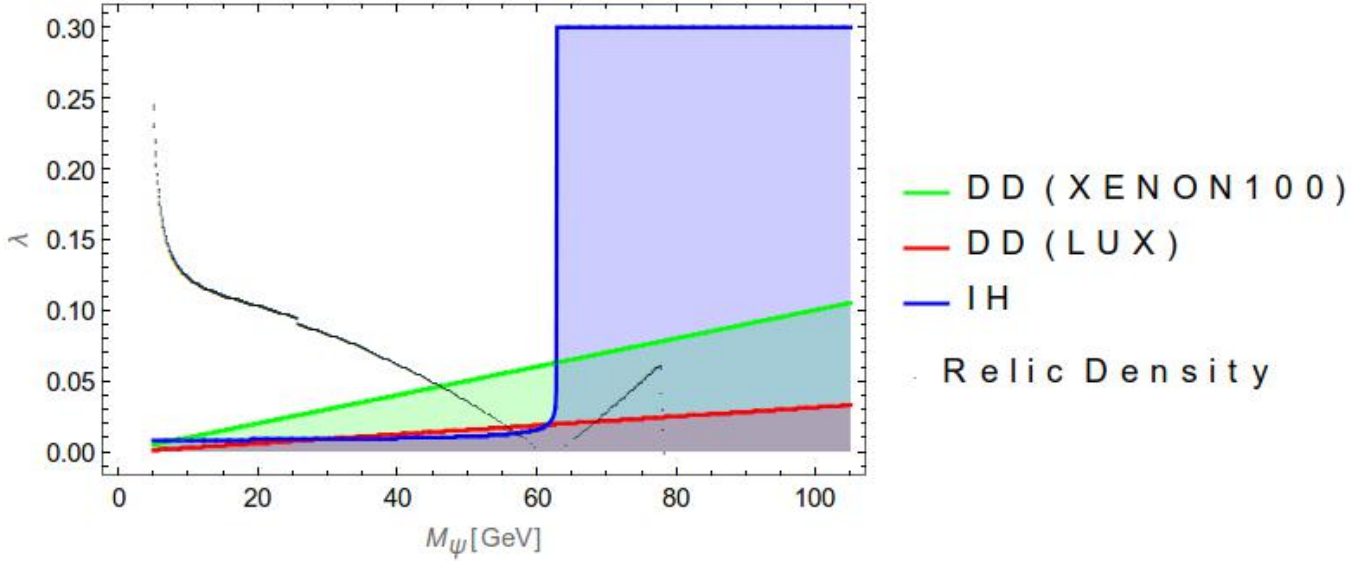


Figure 8: 6HDM at the “symmetric” choice for benchmark point.

we have just one resonance  $M_{H_u} = M_{H_d} = M_H \Rightarrow M_{DM}^{\text{resonance}} = \frac{1}{2}M_H$ , whereas we expect for other choices where  $M_{h_1} \neq M_{h_2}$  to get two resonances.

We also noted a “discontinuity” around the value 30 GeV. However, we traced the origin of this un-smoothness to our method of looping in order to compute  $T_f$ . Upon comparing with other packages (micrOMEGAs) around this point, the smoothness appears, and so the discontinuity is due to numerics and is not physical.

In this work focusing on model building, we carried out all the analytical and numerical analysis using Mathematica packages writing down explicitly the used formulae. In future analysis, more sophisticated DM-oriented programs such as microOMEGAs will be used, and we are currently investigating the case for a more extensive set of benchmark points. Nonetheless, we checked, in a preliminary scan, using micrOMEGAs that Mathematica and micrOMEGAs results are similar. In Fig. (8), we show the micrOMEGAs plot for the “black” relic density constraint, which shows, as expected, less stiffness at the  $Z$ -threshold and more smoothness around the resonance. Moreover, the values of  $\lambda$  satisfying the relic density constraint in the neighborhood of the  $Z$ -threshold get smaller in Fig. 8 compared to Fig. 7. This is justified as micrOMEGAs takes into account the fact that upon increasing the  $DM$  mass, annihilation starts before we reach the threshold [42].

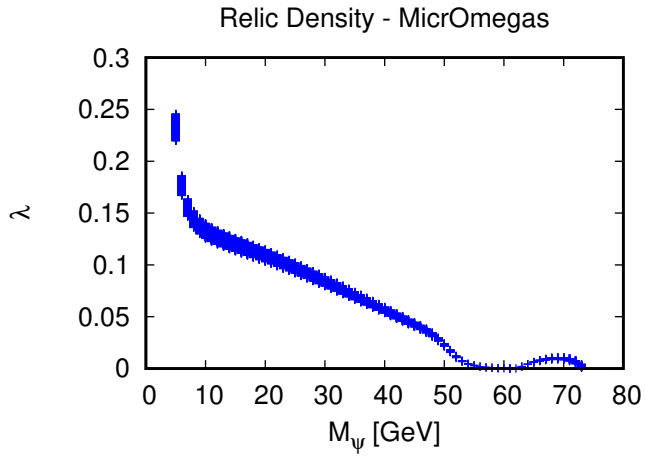


Figure 9: Relic density constraint using micrOMEGAs.

It is noteworthy that the nonstandard interactions between the “new inert” scalars and the “active” Higgses bring about changes  $\Delta S & \Delta T$  to the oblique electroweak parameters  $S, T$  which encode the impact of new physics not coupled to SM fermions [50]. However, this electroweak precision testing goes beyond the scope of this work and will be dealt in the future.

In summary, we presented in this work a non-SUSY extension of the SM, where we have six, instead of one, Higgs doublets. This helps to realize the gauge coupling unification from one part. From the other part, the lightest of the additional Higgs particles presents a suitable candidate for DM. This has been illustrated for a specific benchmark point in the parameter space, and thus should stimulate further investigation for other regions in the parameter space, a systematic full phenomenological analysis of which is a work in progress.

## Acknowledgements

We thank Tianjun Li for useful discussions, and Salah Nasri for reading carefully the manuscript. N.C. wishes to acknowledge support from the CAS PIFI scholarship, and the Humboldt Return fellowship. This work is supported in part by the National Science Foundation of China and by the Chinese Academy of Sciences (the NSFC grant 11375248 for C.L. & C.-S. H., and the NSFC grants 11373030 and 11633004 and CAS grant QYZDJ-SSW-SLH017 for X.C.).

## A 2-loop RGE in 6HDM

In order to derive Eqs. (3–8), we note that the particle content of the 6HDM is just that of the SM plus ( $n_h = 5$ ) new Higgs doublets. Thus, Eq. (2) shows that, at 2-loop order, the 6HDM beta coefficients are just given by:

$$b_k = b_k^{\text{SM}} + b_k^{\text{new}} \quad , \quad b_{k,\ell} = b_{k,\ell}^{\text{SM}} + b_{k,\ell}^{\text{new}} \quad (58)$$

The SM corresponding quantities are known [51]:

$$b_i^{\text{SM}} = \begin{pmatrix} 41/10 \\ -19/6 \\ -7 \end{pmatrix}, b_{ij}^{\text{SM}} = \begin{pmatrix} 199/50 & 27/10 & 44/5 \\ 9/10 & 35/6 & 12 \\ 11/10 & 9/2 & -26 \end{pmatrix}, \quad (59)$$

$$C_{\text{SM}}^u = \begin{pmatrix} -17/10 \\ -3/2 \\ -2 \end{pmatrix}, C_{\text{SM}}^d = \begin{pmatrix} -1/2 \\ -3/2 \\ -2 \end{pmatrix}, C_{\text{SM}}^e = \begin{pmatrix} -3/2 \\ -1/2 \\ 0 \end{pmatrix} \quad (60)$$

We follow [52] to compute the contribution of new physics, and we get:

$$b_k^{\text{new}} = \begin{pmatrix} 1/10 \\ 1/6 \\ 0 \end{pmatrix} \cdot n_h \quad , \quad b_{k,\ell}^{\text{new}} = \begin{pmatrix} 9/50 & 9/10 & 0 \\ 3/10 & 13/6 & 0 \\ 0 & 0 & 0 \end{pmatrix} \cdot n_h \quad (61)$$

Replacing  $n_h = 5$  we get the desired equations. We checked using SARAH that we get the same 2-loop running beta functions for the 6HDM.

## B Mass Eigenstates

### B.1 Tadpole Equations

We get a local minima of  $V_{\text{Active}}$  at  $\phi_u = v_u, \phi_v = v_d$  when

$$\mu_{uu} = -\frac{1}{2}\lambda_{uuuu}v_u^2 - \frac{1}{2}v_d^2(\eta_{uddu} + \lambda_{uudd} + \xi_{udud}) \quad (62)$$

$$\mu_{dd} = -\frac{1}{2}\lambda_{dddd}v_d^2 - \frac{1}{2}v_u^2(\eta_{uddu} + \lambda_{uudd} + \xi_{udud}) \quad (63)$$

## B.2 Mass Matrices

### B.2.1 Mass Matrices for Scalars

1. **Mass matrix for Higgs** , Basis:  $(\phi_u, \phi_d), (\phi_u, \phi_d)$

$$m_h^2 = \begin{pmatrix} \lambda_{uuuu} v_u^2 & v_d v_u (\eta_{uddu} + \lambda_{uudd} + \xi_{udud}) \\ v_d v_u (\eta_{uddu} + \lambda_{uudd} + \xi_{udud}) & \lambda_{dddd} v_d^2 \end{pmatrix} \quad (64)$$

The mass spectrum will read:

$$M_{h_1, h_2}^2 = \frac{1}{4} \left[ (m_h^2)_{11} + (m_h^2)_{22} \pm \sqrt{((m_h^2)_{11} - (m_h^2)_{22})^2 + 4((m_h^2)_{12})^2} \right] \quad (65)$$

This matrix is diagonalized, with mass eigenstates  $(h_1, h_2)$ , by  $Z^H = \begin{pmatrix} \cos \alpha & -\sin \alpha \\ \sin \alpha & \cos \alpha \end{pmatrix}$  with

$$\sin 2\alpha = \frac{2(m_h^2)_{12}}{\sqrt{((m_h^2)_{11} - (m_h^2)_{22})^2 + 4(m_h^2)_{12}^2}} \quad (66)$$

$$\cos 2\alpha = \frac{(m_h^2)_{11} - (m_h^2)_{22}}{\sqrt{((m_h^2)_{11} - (m_h^2)_{22})^2 + 4(m_h^2)_{12}^2}} \quad (67)$$

2. **Mass matrix for Pseudo-Scalar Higgs** , Basis:  $(\sigma_u, \sigma_d), (\sigma_u, \sigma_d)$

$$m_{A^0}^2 = -\xi_{udud} \begin{pmatrix} v_d^2 & -v_d v_u \\ -v_d v_u & v_u^2 \end{pmatrix} \quad (68)$$

with squared mass of the non-Goldstone particle given by

$$M_o^2 = -\xi_{udud} (v_d^2 + v_u^2) \quad (69)$$

This matrix is diagonalized, with mass eigenstates  $(A_1^0, A_2^0)$ , by  $Z^A = \begin{pmatrix} \cos \beta & -\sin \beta \\ \sin \beta & \cos \beta \end{pmatrix}$

3. **Mass matrix for Charged Higgs** , Basis:  $(H_u^{+,*}, H_d^-), (H_u^+, H_d^{-,*})$

$$m_{H^-}^2 = -\frac{1}{2} (\eta_{uddu} + \xi_{udud}) \begin{pmatrix} v_d^2 & v_d v_u \\ v_d v_u & v_u^2 \end{pmatrix} \quad (70)$$

with squared mass of the non-Goldstone particle given by

$$M_c^2 = -\frac{1}{2} (\xi_{udud} + \eta_{uddu}) (v_d^2 + v_u^2) \quad (71)$$

This matrix is diagonalized, with mass eigenstates  $(H_1^\pm, H_2^\pm)$ , by  $Z^+ = Z^A$

4. **Mass matrix for Inert Higgs** , Basis:  $(\phi_1, \phi_2, \phi_3, \phi_4), (\phi_1, \phi_2, \phi_3, \phi_4)$

$$(m_{h^i}^2)_{\alpha\beta} \equiv m_{\phi_\alpha \phi_\beta} = \mu_{\alpha\beta} + \frac{1}{2} \sum_{I=u,d} v_I^2 (\lambda_{II\alpha\beta} + \eta_{I\alpha\beta I} + \xi_{I\alpha I\beta}) \quad (72)$$

5. **Mass matrix for Inert Pseudo-Scalar Higgs** , Basis:  $(\sigma_1, \sigma_2, \sigma_3, \sigma_4), (\sigma_1, \sigma_2, \sigma_3, \sigma_4)$

$$(m_{A^{i0}}^2)_{\alpha\beta} \equiv m_{\sigma_\alpha \sigma_\beta} = \mu_{\alpha\beta} + \frac{1}{2} \sum_{I=u,d} v_I^2 (-\xi_{I\alpha I\beta} + \eta_{I\alpha\beta I} + \lambda_{II\alpha\beta}) \quad (73)$$

6. **Mass matrix for Inert Charged Higgs** , Basis:  $(H_1^+, H_2^+, H_3^+, H_4^+), (H_1^{+,*}, H_2^{+,*}, H_3^{+,*}, H_4^{+,*})$

$$(m_{H^{i+}}^2)_{\alpha\beta} \equiv m_{H_\alpha^+ H_\beta^{+,*}} = \mu_{\alpha\beta} + \frac{1}{2} \sum_{I=u,d} \lambda_{II\alpha\beta} v_I^2 \quad (74)$$

## B.3 Scalar Particle Contents

Name	complex/real	Generations	at “symmetric” benchmark point ( $\beta = 45^\circ = -\alpha, M_{h_1} = M_{h_2}$ )
$h$	real	2	
$A^0$	real	2	$A_1^0 \rightarrow$ goldstone boson, $A_2^0 \rightarrow$ heavy
$H^-$	complex	2	$H_1^- \rightarrow$ goldstone boson, $H_2^- \rightarrow$ heavy
$h^i$	real	4	$h_1^i \rightarrow$ Dark Matter Candidate $\equiv \psi$ , $h_\alpha^i \rightarrow$ heavy where $\alpha = 2, 3, 4$
$A^{i0}$	real	4	$A_\alpha^{i0} \rightarrow$ heavy where $\alpha = 1, 2, 3, 4$
$H^{i+}$	complex	4	$H_\alpha^{i+} \rightarrow$ heavy where $\alpha = 1, 2, 3, 4$

## C Annihilation amplitudes

- $\psi\psi \rightarrow W^+W^-$  Channel:

$$|\mathcal{M}|^2 = \frac{(-4SM_W^2 + 12M_W^4 + S^2)(-g_2^2M_H^2 + g_2^2S + 4\lambda M_W^2)^2}{16M_W^4(S - M_H^2)^2} \quad (75)$$

- $\psi\psi \rightarrow ZZ$  Channel:

$$|\mathcal{M}|^2 = \frac{(-4SM_Z^2 + 12M_Z^4 + S^2)\sec^4(\theta_W)(-g_2^2M_H^2 + g_2^2S + 4\lambda M_W^2)^2}{16M_Z^4(S - M_H^2)^2} \quad (76)$$

- $\psi\psi \rightarrow HH$  Channel:

$$|\mathcal{M}_{h_1 h_1}|^2 = \left( \lambda - \frac{12\lambda M_H^2 M_W^2}{g_2^2 v^2 (M_H^2 - S)} \right)^2 \quad (77)$$

$$|\mathcal{M}_{h_2 h_2}|^2 = \lambda^2 \left( \frac{4M_W^2 \left( \frac{3M_H^2}{v^2(S - M_H^2)} + \lambda \left( \frac{1}{T - M_\psi^2} + \frac{1}{U - M_\psi^2} \right) \right)}{g_2^2} + 1 \right)^2 \quad (78)$$

and we get upon integration over the phase space:

$$\begin{aligned} \omega(S) = & \frac{16\lambda^2 M_W^2}{g_2^4} \left( \frac{\lambda \log \left( \frac{S - 2M_H^2 - \sqrt{S - 4M_H^2} \sqrt{S - 4M_\psi^2}}{S - 2M_H^2 + \sqrt{S - 4M_H^2} \sqrt{S - 4M_\psi^2}} \right) M_H^2 (4M_W^2 (3S + \lambda v^2) - 3g_2^2 S v^2)}{v^2 \sqrt{S - 4M_H^2} (-3S M_H^2 + 2M_H^4 + S^2) \sqrt{S - 4M_\psi^2}} \right. \\ & + \frac{2\lambda \log \left( \frac{S - 2M_H^2 - \sqrt{S - 4M_H^2} \sqrt{S - 4M_\psi^2}}{S - 2M_H^2 + \sqrt{S - 4M_H^2} \sqrt{S - 4M_\psi^2}} \right) M_H^4 (g_2^2 v^2 - 12M_W^2)}{v^2 \sqrt{S - 4M_H^2} (-3S M_H^2 + 2M_H^4 + S^2) \sqrt{S - 4M_\psi^2}} \\ & + \frac{\lambda \log \left( \frac{S - 2M_H^2 - \sqrt{S - 4M_H^2} \sqrt{S - 4M_\psi^2}}{S - 2M_H^2 + \sqrt{S - 4M_H^2} \sqrt{S - 4M_\psi^2}} \right) S v^2 (g_2^2 S - 4\lambda M_W^2)}{v^2 \sqrt{S - 4M_H^2} (-3S M_H^2 + 2M_H^4 + S^2) \sqrt{S - 4M_\psi^2}} \\ & \left. + \frac{3M_H^2 (M_H^2 (6M_W^2 - g_2^2 v^2) + g_2^2 S v^2)}{v^4 (S - M_H^2)^2} + \frac{2\lambda^2 M_W^2}{-4M_H^2 M_\psi^2 + M_H^4 + S M_\psi^2} + \frac{1}{8M_W^2} \right) \end{aligned} \quad (79)$$

- $\psi\psi \rightarrow e^+e^-$  Channel:

$$|\mathcal{M}|^2 = \frac{2\lambda^2 M_e^2 (S - 4M_e^2)}{(S - M_H^2)^2} \quad (80)$$

---

- $\psi\psi \rightarrow u\bar{u}$  Channel:

$$|\mathcal{M}|^2 = \frac{6\lambda^2 M_u^2 (S - 4M_u^2)}{(S - M_H^2)^2} \quad (81)$$

---

- $\psi\psi \rightarrow d\bar{d}$  Channel:

$$|\mathcal{M}|^2 = \frac{6\lambda^2 M_d^2 (S - 4M_d^2)}{(S - M_H^2)^2} \quad (82)$$

---

## D Direct Detection Amplitudes

$$|\mathcal{M}|^2 = -\frac{3\lambda^2 M_N^2 \eta_N^2 (T - 4M_N^2)}{(T - M_H^2)^2} \quad (83)$$

The thermal average for total scattering:

$$\langle \sigma v_{rel} \rangle = \frac{12\lambda^2 M_N^4 \eta_N^2}{M_H^4} + \frac{6\lambda^2 p_f^2 M_N^2 \eta_N^2 (M_H^2 - 8M_N^2)}{M_H^6} + O(p_f^3) \quad (84)$$

## E Invisible Higgs Decay

- $h_i \rightarrow f\bar{f}$

$$|\mathcal{M}|^2 = \frac{C_f g_f^2 M_f^2 (M_H^2 - 4M_f^2)}{4M_W^2} \quad (85)$$

where:

$f = u, d, e$  &  $i = 1, 2$

$C_f = 1$  for leptons

$C_f = 3$  for quarks

---

- $h_2 \rightarrow ZZ$

$$|\mathcal{M}|^2 = \frac{g_2^2 M_W^2 (-4M_H^2 M_Z^2 + M_H^4 + 12M_Z^4) \sec^4(\theta_W)}{4M_Z^4} \quad (86)$$

---

- $h_2 \rightarrow W^+W^-$

$$|\mathcal{M}|^2 = \frac{g_2^2 (-4M_H^2 M_W^2 + M_H^4 + 12M_W^4)}{4M_W^2} \quad (87)$$

---

- $h_2 \rightarrow \psi_k \psi_j$

$$|\mathcal{M}|^2 = \frac{4\lambda^2 M_W^2}{g_2^2} \quad (88)$$

## F self Elastic Scattering Amplitudes

$$|\mathcal{M}|^2 = \left( \frac{4\lambda^2 M_W^2 \left( \frac{1}{S-M_H^2} + \frac{1}{T-M_H^2} + \frac{1}{U-M_H^2} \right)}{g_2^2} + \lambda_S \right)^2 \quad (89)$$

The total scattering:

$$\begin{aligned} \langle \sigma_{el} \rangle = & \frac{\left( g_2^2 M_H^4 \lambda_s - 4M_H^2 \left( g_2^2 M_\psi^2 \lambda_s + 3\lambda^2 M_W^2 \right) + 32\lambda^2 M_W^2 M_\psi^2 \right)^2}{g_2^4 M_H^4 \left( M_H^2 - 4M_\psi^2 \right)^2} \\ & - \frac{256 p_f^2 \left( \lambda^2 M_W^2 M_\psi^2 \left( M_H^2 - 2M_\psi^2 \right) \left( g_2^2 M_H^4 \lambda_s - 4M_H^2 \left( g_2^2 M_\psi^2 \lambda_s + 3\lambda^2 M_W^2 \right) + 32\lambda^2 M_W^2 M_\psi^2 \right) \right)}{g_2^4 M_H^6 \left( M_H^2 - 4M_\psi^2 \right)^3} \\ & + O(p_f^3) \end{aligned} \quad (90)$$

## References

- [1] Planck Collaboration, A&A, 594 (2016),
- [2] C. Patrignani et al. (Particle Data Group), Chin. Phys. C, 40, 100001 (2016) and 2017 update
- [3] S. Dimopoulos, S. Raby and F. Wilczek, Phys. Rev. D **24**, 1681 (1981).
- [4] H. Murayama and A. Pierce, Phys.Rev.D65:055009,2002
- [5] P. Nath and P. F. Perez, Phys.Rept.441:191-317, 2007 (see section 4.5).
- [6] S. Willenbrock, Phys. Lett. B **561**, 130 (2003).
- [7] K. S. Babu, X. G. He and S. Pakvasa, Phys. Rev. D **33**, 763 (1986),  
A. de Rujula, H. Georgi and S.L. Glashow, in "Fifth Workshop on Grand Unification", edit by K. Lang, H. Fried and P. Framton, World Scientific (1984) p.88
- [8] J. Sayre, S. Wiesenfeldt and S. Willenbrock, Phys. Rev. D **73**, 035013 (2006).
- [9] M. S. Turner, Phys. Rept. 197, 6797 (1990);  
G. G. Raffelt, Phys. Rept. 198, 1113 (1990).
- [10] B. W. Lee and S. Weinberg, Phys. Rev. Lett. **39**, 165 (1977).
- [11] I. Antoniadis, Phys. Lett. B **246**, 377 (1990);  
H. C. Cheng, K. T. Matchev and M. Schmaltz, Phys. Rev. D **66**, 056006 (2002).
- [12] J. A. R. Cembranos, A. Dobado and A. L. Maroto, Phys. Rev. Lett. **90**, 241301 (2003).
- [13] C. P. Burgess, M. Pospelov and T. t. Veldhuis, Nucl. Phys. B **619**, 709 (2001).
- [14] A. Abada and S. Nasri, Phys. Rev. D **83** (2011) 095021.
- [15] E. Ma, Phys. Rev. D **73**, 077301 (2006)
- [16] R. Barbieri, L. J. Hall and V. S. Rychkov, Phys. Rev. D **74**, 015007 (2006)
- [17] A. Alves, D. A. Camargo, A. G. Dias, R. Longas, C. C. Nishi and F. S. Queiroz, J. High Energ. Phys. (2016) 2016: 15.  
F. S. Queiroz and C. E. Yaguna, JCAP02(2016)038
- [18] L. L. Honorez, E. Nezri, J. F. Oliver and M. H.G. Tytgat, JCAP **0702**, 028 (2007).

- [19] E.M. Dolle and S. Su, Phys. Rev. D 80, 055012 (2009)
- [20] T.D. Lee, PRD **8**, 1226 (1973),  
S.L. Glashow and S. Weinberg, Phys. Rev. D **15**, 1958 (1977)  
J.F. Gunion and H.E. Haber, Phys. Rev. D 67, 075019 (2003).
- [21] H. E. Haber, G. L. Kane and T. Sterling, Nucl. Phys. B. **161**, 493 (1979).  
J. F. Donoghue and L. F. Li, Phys. Rev. D. **19**, 945 (1979).  
L. F. Abbott, P. Sikivie and M. B . Wise, Phys. Rev. D. **21**, 1393 (1980).
- [22] G.C. Branco, P.M. Ferreira, L. Lavoura, M.N. Rebelo, M. Sher and J. P. Silva, Phys. Rep. Volume 516 (2012), 1.
- [23] C.-S. Huang, L. Wei, Q.-S. Yan, S.-H. Zhu, Phys.Rev. D**63** (2001) 114021, Erratum: Phys.Rev. D**64** (2001) 059902,  
C.-S. Huang and S.-H. Zhu, Phys.Rev. D**61** (2000) 015011, Erratum: Phys.Rev. D**61** (2000) 119903,
- [24] V. Keus, S. F. King and S. Moretti, Phys. Rev. D 90, 075015 (2014)
- [25] V. Keus, S. F. King, S. Moretti and D. Sokolowska, High Energ. Phys. (2014) 2014: 16.
- [26] H.E. Haber, Talk given at the "Toyama International Workshop on Higgs as a Probe of New Physics 2013, arXiv: 1401.0152
- [27] G. Bhattacharyya and D. Das, Pramana - J Phys (2016) 87: 40. , arXiv:1507.06424
- [28] B. Grzadkowski, O.M. Ogreid, P. Osland, A. Pukhov and M. Purmohammadi, JHEP **1106** (2011) 003.
- [29] <https://sarah.hepforge.org/> ;  
F. Staub, Computer Physics Communications 185 (2014) pp. 1773-1790 ;  
<http://www.feynarts.de/> ;  
<http://www.feynarts.de/formcalc/>.
- [30] E. W. Kolb and M. S. Turner, The Early Universe, Addison-Wesley (1990).
- [31] T. Falk, K. A. Olive and M. Srednicki, Phys.Lett.B339:248-251,1994
- [32] <https://lapth.cnrs.fr/micromegas/>
- [33] A. G. Dias and V. Pleitez, Phys.Rev. D70 (2004) 055009
- [34] S. Weinberg, Phys. Rev. Lett. **37**, 657 (1976).
- [35] K. Shizuya, S.-H. H. Tye, Phys. Rev. **D23**, 1613 (1981).
- [36] N.G. Deshpande and E. Ma, Phys. Rev. **D18**, 2574 (1978).
- [37] See, e.g., ref. [47]; C.-S. Huang, W. Liao, Q.-S. Yan, S.-H. Zhu, Phys. Rev. **D63**, 114021 (2001), Erratum-ibid. **D64**, 059902 (2001).
- [38] P. M. Ferreira, H. E. Haber, R. Santos and J. P. Silva, Phys. Rev. **D87**, 055009 (2013)
- [39] S. Khalil and C. Munoz, Contemp.Phys. 43 (2002) 51-62
- [40] M. Srednicki, R. Watkins and K. A. Olive, Nucl. Phys. B **310**, 693 (1988).
- [41] T. Falk, K. A. Olive and M. Srednicki, Phys. Lett. B **339**, 248 (1994).
- [42] P. Gondolo and G. Gelmini, Nuclear Physics B360 (1991) 145-179
- [43] LUX collaboration, Phys. Rev. Lett. 118, 021303 (2017)

- [44] Xenon100 collaboration, Phys. Rev. D 94, 122001 (2016)
- [45] S. Bhattacharya, P. Ghosh, T. N. Maity and T. S. Ray, arXiv:1706.04699
- [46] R. Garani and S. Palomares-Ruiz, JCAP 1705 (2017) no.05, 007
- [47] J.F. Gunion, H.E. Haber, G. Kane and S. Dawson, The Higgs Hunter's Guide, *Frontiers in Physics*, Addison-Wesley 1990
- [48] B. Moore *et al.*, *M.N.R.A.S.* **310** (1999) 1147, *Ap. J.* **524** (1999) L19; A. A. Klypin *et al.*, *Ap. J.* **522** (1999) 82, *Ap. J.* **554** (2001) 903.
- [49] K.A. Olive et al. (Particle Data Group), Chin. Phys. C, 38 , 090001 (2014) and 2015 update
- [50] A. Ahriche, G. Faisel, S. Nasri and J. Tandean, Nucl. Phys. B 916 (2017) 64-93
- [51] M.E. Machacek and M. T. Vaughn, Nucl. Phys. **B222**, 8 (1983).
- [52] D.R.T. Jones, Phys. Rev. **D25**, 581 (1982)